

## STATIONKEEPING FOR THE LUNAR RECONNAISSANCE ORBITER (LRO)

Mark Beckman<sup>1</sup> and Rivers Lamb<sup>2</sup>

The Lunar Reconnaissance Orbiter (LRO) is scheduled to launch in 2008 as the first mission under NASA's Vision for Space Exploration. Following several weeks in a quasi-frozen commissioning orbit, LRO will fly in a 50 km mean altitude lunar polar orbit. During the one year mission duration, the orbital dynamics of a low lunar orbit force LRO to perform periodic sets of stationkeeping maneuvers. This paper explores the characteristics of low lunar orbits and explains how the LRO stationkeeping plan is designed to accommodate the dynamics in such an orbit. The stationkeeping algorithm used for LRO must meet five mission constraints. These five constraints are to maintain ground station contact during maneuvers, to control the altitude variation of the orbit, to distribute periselene equally between northern and southern hemispheres, to match eccentricity at the beginning and the end of the sidereal period, and to minimize stationkeeping  $\Delta V$ . This paper addresses how the maneuver plan for LRO is designed to meet all of the above constraints.

### INTRODUCTION

The Lunar Reconnaissance Orbiter (LRO) is the first mission under NASA's Vision for Space Exploration. LRO will launch on an Atlas V launch vehicle in late 2008 using a direct minimum energy transfer to reach the moon. The spacecraft has a one year mission duration in a low lunar polar orbit. LRO is a three axis stabilized, nadir-pointing spacecraft with a launch mass of approximately 1900 kg. As shown in Figure 1, the spacecraft will fly seven instruments that will characterize future robotic and human landing sites, identify potential lunar resources, and document lunar radiation relevant to human biological response.

After launch, LRO will spend 4-5 days (depending on launch date) on its transfer trajectory to the moon. When LRO arrives at the moon, a sequence of Lunar Orbit Insertion (LOI) maneuvers are planned that will first capture the spacecraft into lunar orbit and then lower the altitude to a quasi-frozen orbit at 30 x 216 km altitude for commissioning. Commissioning phase will last up to sixty days, ending when all instruments have been checked out and the decision is made to maneuver into the final mission orbit. The mission orbit is a 50 km mean polar orbit, and LRO will remain in this orbit for one year. Figure 2 shows the primary phases of the LRO mission.

---

<sup>1</sup> LRO Flight Dynamics Lead, Goddard Space Flight Center, Code 595, Greenbelt, MD 20771

<sup>2</sup> LRO Flight Dynamics Ground System Lead, Goddard Space Flight Center, Code 595, Greenbelt, MD 20771

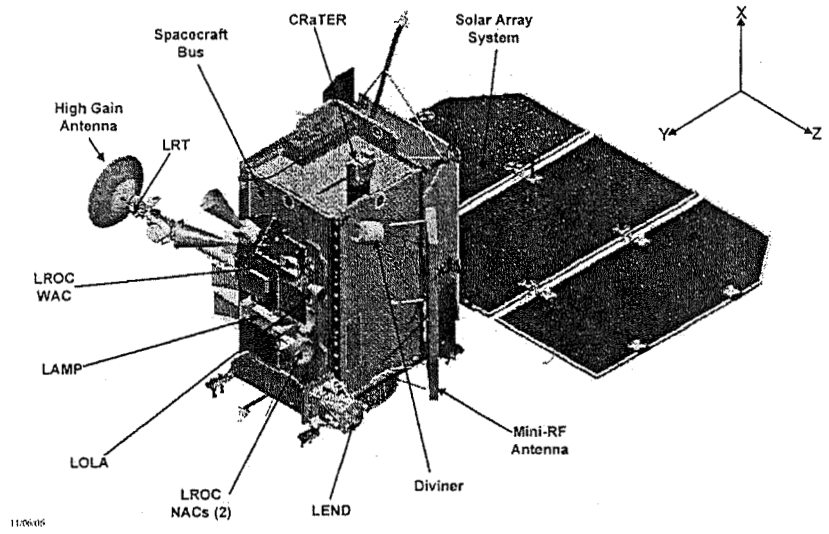


**Figure 1: LRO Spacecraft**

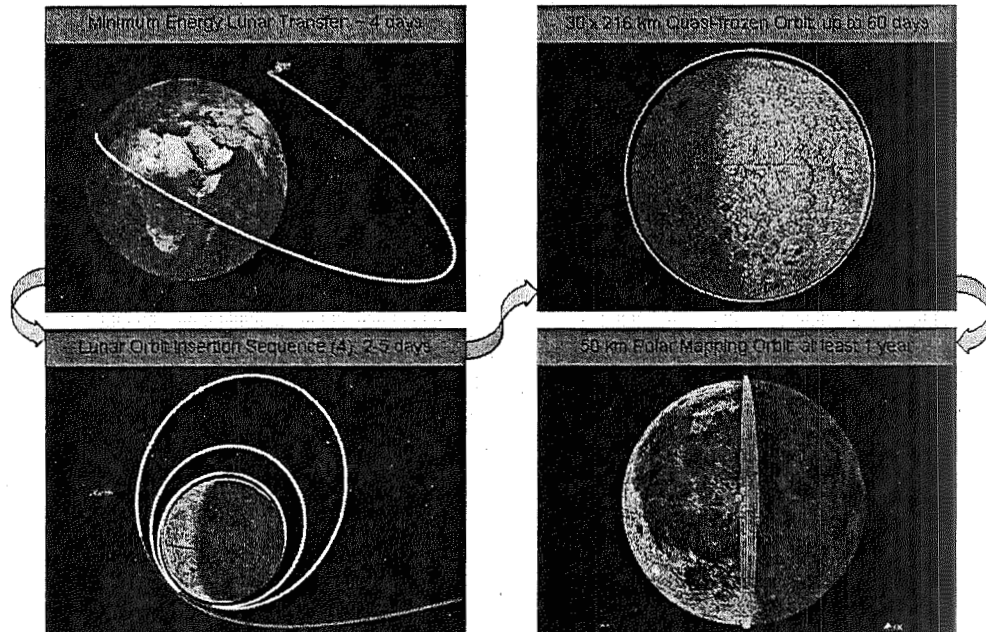


**Figure 2: LRO Mission Phases**

The Flight Dynamics Analysis Branch (FDAB) at the Goddard Space Flight Center (GSFC) will provide all mission design, maneuver planning and orbit determination support for LRO. The FDAB has supported the last two NASA missions to the moon. The FDAB provided launch, maneuver planning, orbit determination and mission design support for Clementine and Lunar Prospector. Clementine was a Naval Research Laboratory mission that flew in 1994 in a highly elliptical lunar orbit. Lunar Prospector (LP) was a Discovery class mission that launched in 1998. LP was in a low polar lunar mapping orbit at 100 km altitude for the nominal mission, then at 40 and 30 km for the six month extended mission (Ref. 1).

## LUNAR GRAVITY MODELS

LRO will fly in a low lunar orbit during the nominal mission. In a low lunar orbit, defined as below 100 km in mean altitude, lunar non-spherical gravity is by far the dominant force on the spacecraft and has a dramatic effect on altitude evolution.

The LP mission provided valuable tracking data in low lunar orbits that were used to develop high accuracy lunar gravity models. Alex Konopliv, at the Jet Propulsion Laboratory (JPL), developed the LP100K and LP150Q lunar gravity models (Ref 2). The LP150Q model is the latest model in the series and is considered the most accurate. The LP100K model is the latest model that is limited in degree and order to 100. Table 1 below shows the differences between long term propagations (57 days) using each gravity model.

**Table 1: Comparison of LP100K vs. LP150Q**

| Max R<br>(km) | Max I<br>(km) | Max C<br>(km) | Max Total<br>(km) |
|---------------|---------------|---------------|-------------------|
| 0.20          | 6.86          | 0.14          | 6.86              |

As shown in Table 1, there is no significant difference in the accuracy of these two models, particularly in the radial and cross-track directions. Since the LP100K model is significantly less computationally intensive, this model is used for LRO mission and maneuver planning.

## LONG TERM LUNAR PROPAGATION

LRO will fly in a mean 50 km mission orbit that, for scientific purposes, would ideally be a perfectly circular orbit. Due to the lunar non-spherical gravity, however, long term propagations of low lunar orbits show significant altitude variations and secular drift in periselene and apselene altitudes. In fact, this drift will cause the orbit's periselene altitude to decrease until the spacecraft collides with the surface of the moon. Figure 2 shows a plot of periselene and apselene altitudes versus time starting from a 50 km circular polar orbit. Figures 3 and 4 are the same plots for 100 km and 200 km circular polar orbits respectively. The 50 km orbit is representative of the desired LRO altitude. The 100 km orbit is representative of the desired altitude of the Crew Exploration Vehicle (CEV).

A spacecraft in an initially circular polar orbit about the moon at an altitude of 50 km will impact the Moon in approximately 41 days, assuming an altitude of 12 km for impact – the height of the tallest mountains on the moon. At 100 km altitude, the impact is delayed until about 150 days. At 200 km altitude, impact is avoided as the altitude variations are bounded. Therefore, a 200 km orbit is valuable since stationkeeping costs are eliminated. For orbits at 100 km and below, stationkeeping maneuvers are required to maintain altitude control.

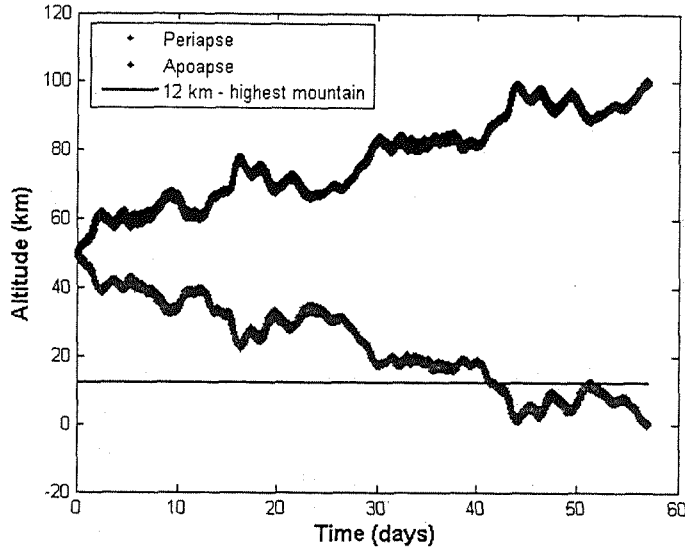


**Figure 2: Altitude Variation for 50 km Orbit**

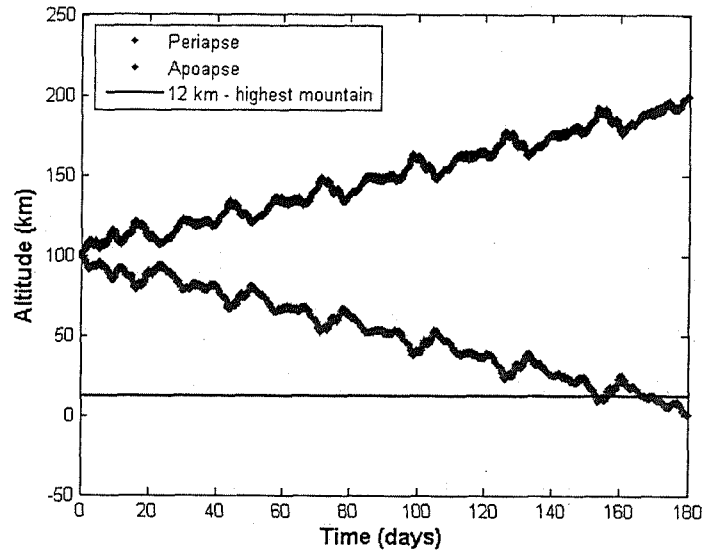


**Figure 3: Altitude Variation for 100 km Orbit**

### LUNAR PHASE PLOTS

The altitude variations shown in Figures 2-4 indicate a periodic component to the altitude evolution. Analysis has shown that semi-major axis ( $a$ ), inclination ( $i$ ) and right ascension of the ascending node ( $\Omega$ ) do not vary significantly over time. However, argument of periapsis ( $\omega$ ) does. Since altitude varies significantly, obviously so does eccentricity ( $e$ ). This suggests that a more informative relationship is that between  $e$  and  $\omega$  (Ref. 3). Figures 5-7 show the same propagations shown in Figures 2-4, but in the defined  $e$  vs.  $\omega$  phase plot. In each plot, the evolution of the orbit moves from the center of the plot ( $e = 0$ ) to the right.

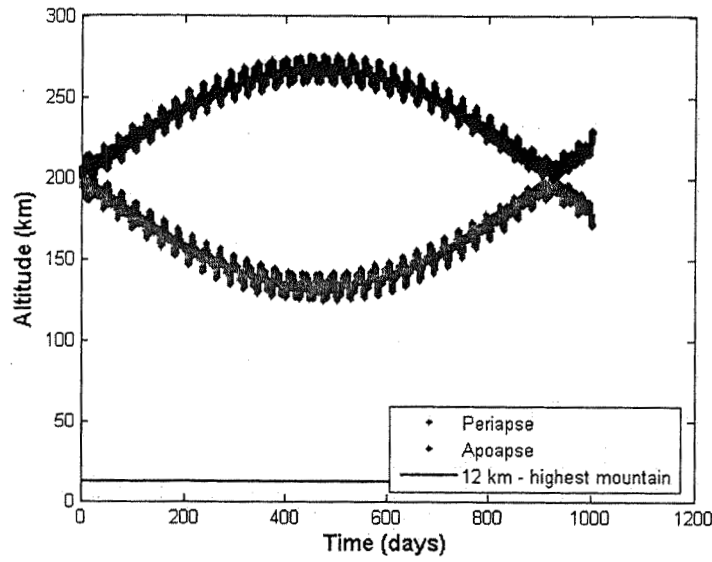


**Figure 4: Altitude Variation for 200 km Orbit**

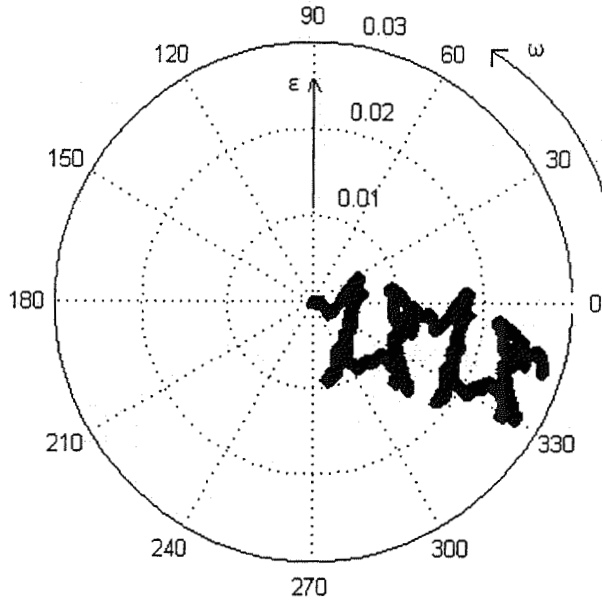


**Figure 5: Phase Plot for 50 km Orbit**

Three important characteristics can be observed in these phase plots. First, the motion of  $e$  vs.  $\omega$  is highly irregular. Next, this irregular pattern is repeated at a frequency equal to the lunar sidereal period, or approximately every 27.4 days. Finally, the evolution seems to encircle a point on the  $e$  vs.  $\omega$  phase plot. This unique point will be discussed later.

In Figures 5 and 6, the propagations stop when  $e$  approaches a particular value. Given a constant semi-major axis, the increasing value of  $e$  is equivalent to a decreasing periselene altitude. As mentioned previously, 12 km is used as the altitude at which the

spacecraft is in danger of impacting the high lunar mountains. For the 50 km orbit, this 12 km altitude limit corresponds to an  $e$  limit of 0.021, and for the 100 km orbit, this corresponds to an  $e$  limit of 0.048.

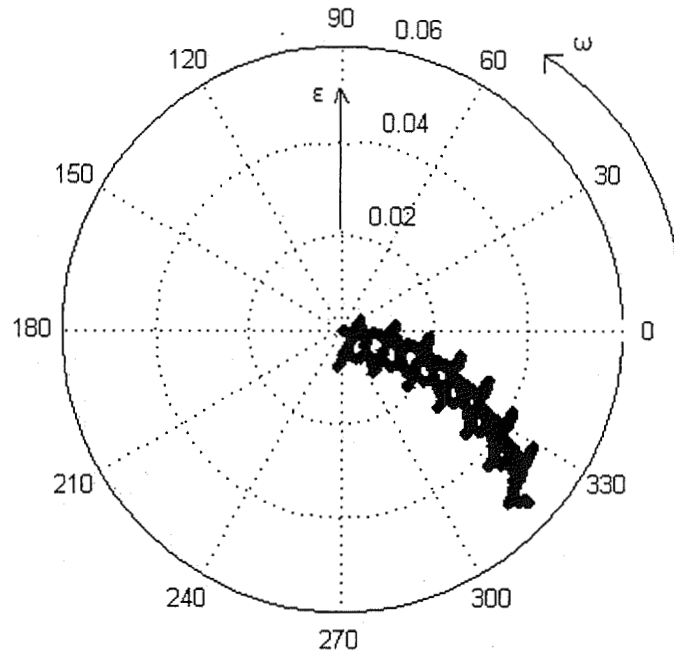


**Figure 6: Phase Plot for 100 km Orbit**

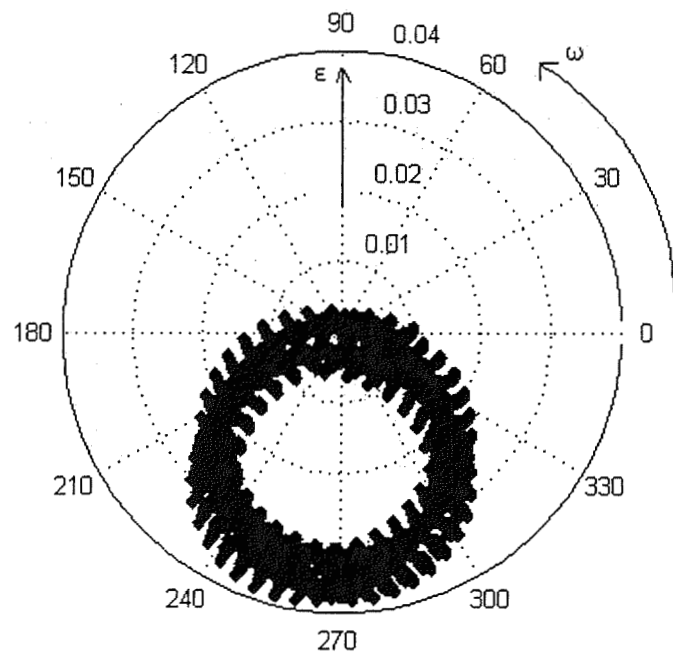


**Figure 7: Phase Plot for 200 km Orbit**

In Figure 7, the propagation does not stop at a particular value of  $e$ . In a 200 km orbit, the spacecraft would not approach the altitude limit of 12 km until the value for  $e$  reached 0.097. Figure 7 shows that  $e$  never gets above 0.04, so the evolution is allowed to completely close upon itself. Therefore, an orbit with this semi-major axis would be a safe orbit with no possibility of lunar impact.

Another important observation from these three figures is that the center of the pattern of evolution is different for each of the three cases. At 50 km altitude, the center of the radius of curvature is about  $e = 0.042$  (though this is hard to confirm from Figure 5). At 100 km, the center of the radius of curvature is about  $e = 0.032$ . At 200 km, the center of the radius of curvature is about  $e = 0.027$ . In all cases, the center is very near  $\omega = 270$  deg. These results are discussed in more detail later in the section on frozen orbits.

### TRANSLATION THEOREM

Focusing on the 50 km altitude phase plot (Figure 5), it is apparent that the pattern generated by one lunar sidereal period is very close to the pattern generated by the second period. The first pattern had initial conditions of  $e = \omega = 0$ , and the second pattern had initial conditions of  $e \sim 0.015$  and  $\omega \sim 350$  deg. Yet both patterns are remarkably similar. This suggests that the  $e$  vs.  $\omega$  pattern, for this  $a$  and  $i$ , is independent of initial conditions. In Figure 8, we test this theorem. Four sets of initial conditions are shown, all within an  $e < 0.02$ . Each initial condition is propagated for one lunar sidereal period.

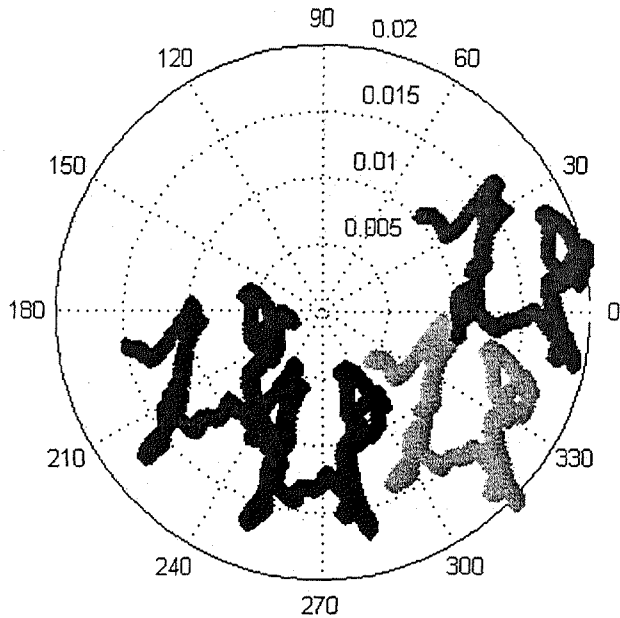


**Figure 8: Test of Translation Theorem**

Figure 8 shows that each  $e$  vs.  $\omega$  pattern, while not identical, is, to first order, the same. This characteristic of the  $e$  vs.  $\omega$  pattern can then be used to develop a stationkeeping algorithm. By translating the  $e$  vs.  $\omega$  pattern to any desired location in the  $e$  vs.  $\omega$  phase

plot,  $e$  can be bounded to a very small number. Then, with stationkeeping maneuvers used to reset the initial conditions each lunar sidereal period, the  $e$  vs.  $\omega$  pattern can simply be repeated ad infinitum to provide altitude control.

## LRO STATIONKEEPING REQUIREMENTS

LRO has five constraints on the stationkeeping algorithm used as listed below:

1. Maintain ground station contact during stationkeeping maneuvers
2. Control altitude to within 20 km of the mean 50 km altitude
3. Control periselene to spend at least 48% of the time in each of the northern and southern hemispheres
4. Match orbit eccentricity at the beginning and the end of the period
5. Minimize stationkeeping  $\Delta V$

First, stationkeeping maneuvers should occur such that there is ground station contact with the spacecraft during the maneuvers. In low lunar orbit, the spacecraft is often occulted by the moon. The geometry of LRO's orbit plane relative to the Earth is described by the beta-Earth angle. When the Earth is in the lunar orbit plane, the beta-Earth angle is defined to be zero. Therefore, when the beta-Earth angle is 90 deg, the entire lunar orbit is visible from the Earth. Since the prime meridian of the moon is through the mean-sub-Earth point, the Lunar Longitude of the Ascending Node (LLAN) of this 90 deg beta-Earth angle is always approximately 90 or 270 deg.

The points in the above phase plots can be associated with a particular LLAN, effectively describing the location of the ascending node of the orbit relative to the surface of the moon. Figure 9 adds LLAN data to the phase plot to show how LLAN is linked to the  $e$  vs.  $\omega$  evolution. The LLAN values are shown next to the phase plot every 10 deg in LLAN. The  $e$  vs.  $\omega$  pattern for one lunar sidereal period can be broken in one of two places – at either a LLAN of 90 or 270 deg. This creates two possible repeated  $e$  vs.  $\omega$  patterns each cycle. Both patterns meet the requirement that the stationkeeping maneuvers are visible to ground stations, so the choice between these two patterns is made based upon other factors. Figure 10 shows both possible  $e$  vs.  $\omega$  patterns.

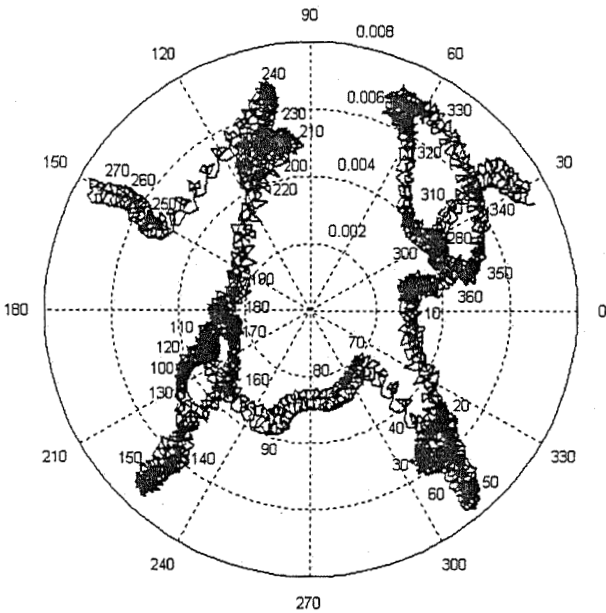


**Figure 9: LLAN vs.  $e$  vs.  $\omega$  pattern**

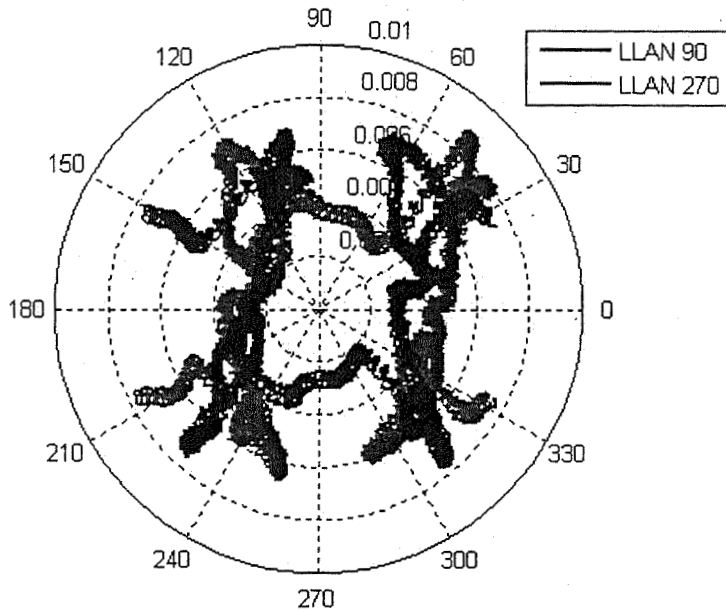


**Figure 10: Two  $e$  vs.  $\omega$  Patterns: 90 & 270 deg LLAN**

In a perfectly circular orbit, LRO would be able to collect uniform science data. As previously shown, that is not possible, and the next step is to control the altitude variation. LRO instrument principal investigators have agreed to a  $\pm 20$  km altitude variation requirement. At a 50 km mean altitude, this translates to a maximum eccentricity of 0.0112. Both of the repeating patterns shown in Figure 10 exist entirely within the eccentricity circle of 0.0112, so altitude will be controlled even tighter than the science requirement.

If the  $e$  vs.  $\omega$  pattern is translated solely to fit within the smallest eccentricity circle, the periselene will spend more time in either the northern or southern hemisphere, depending on whether the 90 or 270 LLAN pattern is chosen. The LRO scientists desire a more consistent distribution of periselene in the northern and southern hemispheres. Therefore, after translating the  $e$  vs.  $\omega$  pattern to fit within the smallest eccentricity circle, the  $e$  vs.  $\omega$  pattern is then translated north/south so that periselene spends at least 48% of the time in each hemisphere. This translation will increase the maximum eccentricity of the cycle.

After the  $e$  vs.  $\omega$  pattern is centered north/south, the initial and final conditions of the repeating pattern are compared. If the eccentricity of the initial and final states match, then the stationkeeping maneuver used to jump back to the start of the pattern is a simple optimized line-of-apsides rotation. This two-burn sequence makes the stationkeeping maneuvers similar in size and at a fixed separation in time. In order to perform an optimized line-of-apsides maneuver, the eccentricities of the initial and final states must match. The  $e$  vs.  $\omega$  pattern is translated east/west until the eccentricities match. This translation will also increase the maximum eccentricity of the cycle.

Finally, stationkeeping  $\Delta V$  costs must be minimized. Stationkeeping  $\Delta V$  cost is the final determining factor in choosing between acceptable stationkeeping strategies. Figure 11 shows the  $e$  vs.  $\omega$  pattern as the pattern is translated for each of the LRO stationkeeping requirements.

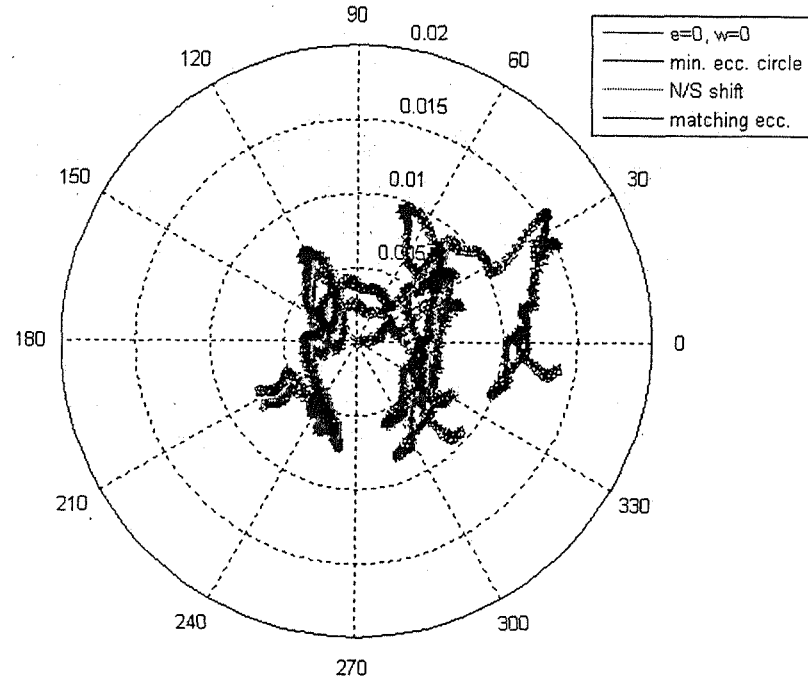


**Figure 11: Application of LRO Stationkeeping Requirements on  $e$  vs.  $\omega$  Pattern**

## LRO STATIONKEEPING OPTIONS

Given the constraints above, there are several options for the stationkeeping maneuvers. The line-of-apsides maneuver can be performed in one of two ways - the semi-major axis of the transfer orbit between the initial and final orbits can be higher or lower than the semi-major axis of the initial and final orbits. Additionally, the repeating  $e$  vs.  $\omega$  pattern can be broken at either 90 or 270 degrees LLAN. This gives a total of four different options that all meet the first four LRO stationkeeping requirements. Figures 12-15 show each of these four options, including the stationkeeping maneuvers used to reset the pattern. Table 2 compares these four options.

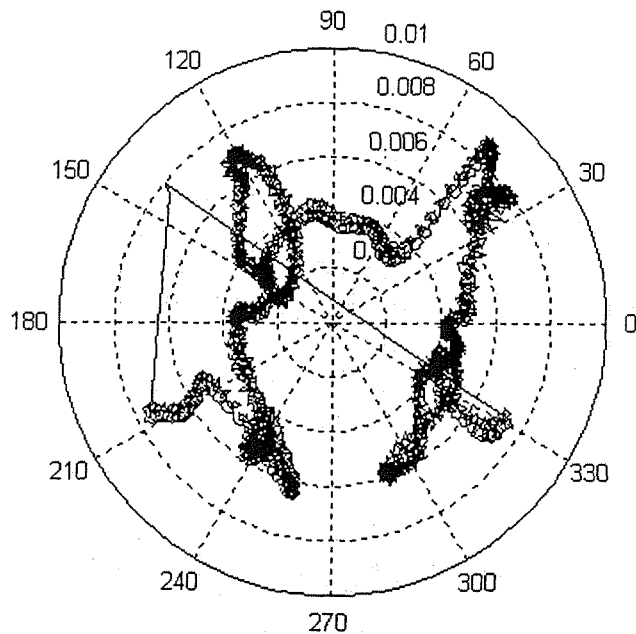
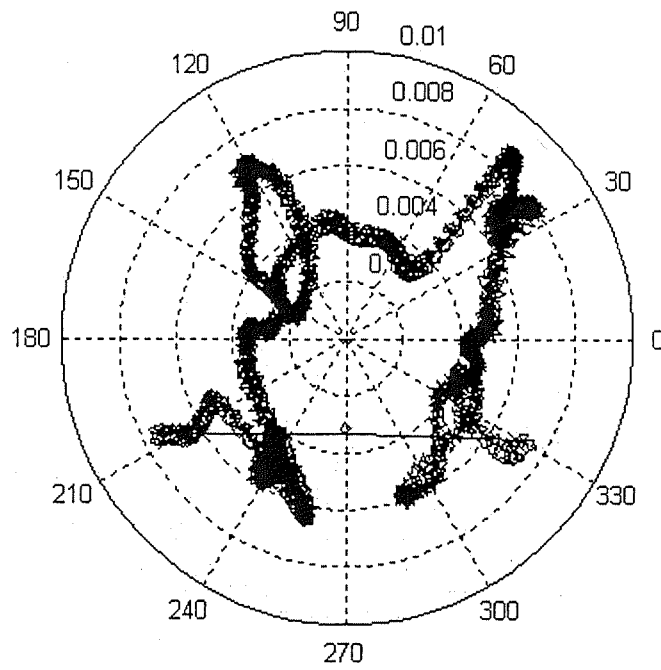
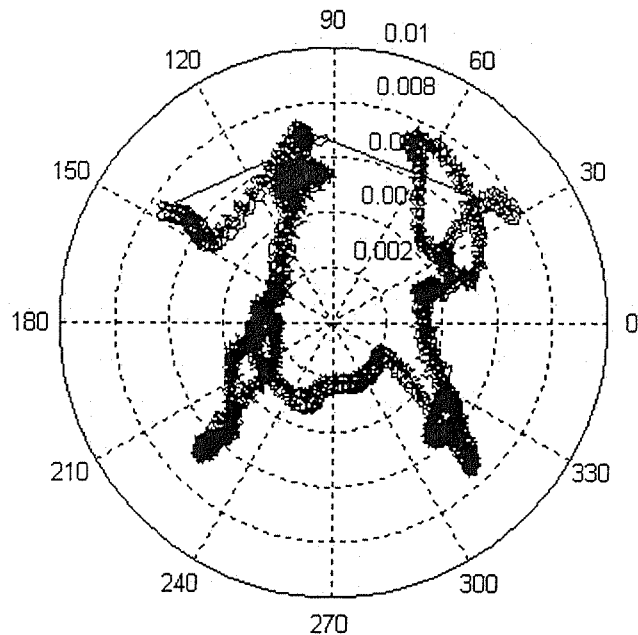


Figure 12: Stationkeeping Algorithm: 90 deg LLAN, Low Transfer

Using the data above, it is possible to determine the optimal stationkeeping sequence based on the five constraints for LRO. Four of the constraints have been met by all four transfer options, as each option maintains ground contact during maneuvers, controls altitude to within 20 km, distributes periselene equally, and matches orbit eccentricity at the beginning and end of the period. The fifth constraint, minimize stationkeeping  $\Delta V$ , leads the analyst to eliminate both of the low transfer options. The two high transfer options are nearly identical in  $\Delta V$  costs, but the LLAN = 270 deg case is chosen since it also provides the smallest altitude variation during each sidereal period.



**Figure 13:** Stationkeeping Algorithm: 90 deg LLAN, High Transfer



**Figure 14:** Stationkeeping Algorithm: 270 deg LLAN, Low Transfer

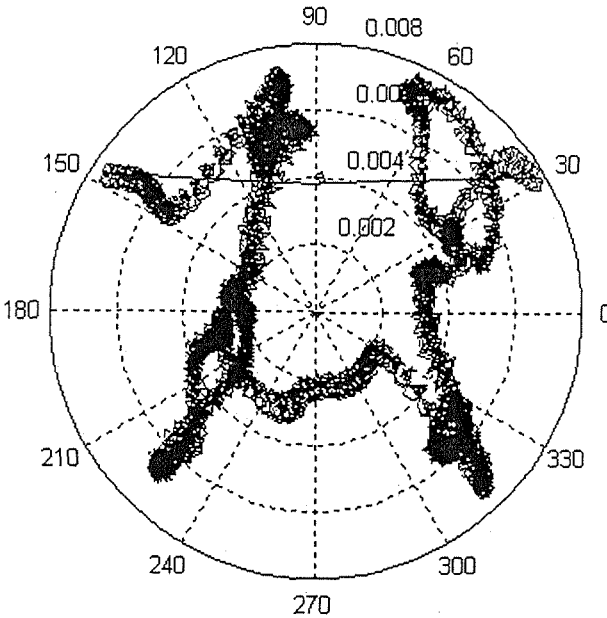


**Figure 15:** Stationkeeping Algorithm: 270 deg LLAN, High Transfer

**Table 2: Stationkeeping Algorithm Comparison**

| LLAN | Transfer Type | $\Delta V 1$ (m/s) | $\Delta V 2$ (m/s) | Total $\Delta V$ (m/s) | Maximum Eccentricity | Altitude Variation (km) |
|------|---------------|--------------------|--------------------|------------------------|----------------------|-------------------------|
| 90°  | High          | 5.29               | 5.56               | 10.84                  | 0.00890              | 15.91                   |
| 90°  | Low           | 12.52              | 6.66               | 19.18                  | 0.00886              | 15.83                   |
| 270° | High          | 5.46               | 5.34               | 10.81                  | 0.00792              | 14.16                   |
| 270° | Low           | 6.53               | 5.45               | 11.98                  | 0.00803              | 14.35                   |

### QUASI-FROZEN COMMISSIONING ORBIT

As mentioned previously, Figures 5-7 suggest the existence of a unique set of initial conditions about which the long term  $e$  vs  $\omega$  pattern revolves. Such a condition can be useful, as it would eliminate the need for stationkeeping maneuvers to reset the sidereal pattern. At a low mean altitude such as 50 km, however, the  $e$  required for this condition is too large, as the periselene altitude would not be above the surface of the moon. So the  $a$  for this condition would have to be raised to set a minimum safe periselene altitude.

This type of orbit is described as a quasi-frozen orbit, as the  $e$  vs  $\omega$  pattern is not static but is bounded. While it cannot be used for LRO's mission orbit, the qualities of the quasi-frozen orbit would be useful for LRO's commissioning orbit. The use of the quasi-frozen condition for the commissioning orbit would save stationkeeping  $\Delta V$  costs and allow valuable tracking data to be obtained in this unique orbit. Additional information on lunar frozen orbits is available in Ref. 4.

Since the lowest allowed altitude for LRO during the nominal mission is 30 km, this is used as a guideline to define the lower bound for the mission's quasi-frozen commissioning orbit. Figure 16 shows the evolution of the  $e$  vs  $\omega$  pattern from an initial  $26 \times 216$  km orbit. Note that periselene of the quasi-frozen orbit is about 270 deg or directly over the lunar south pole. This is advantageous since the south pole is of considerable interest for science and as a potential future landing site.

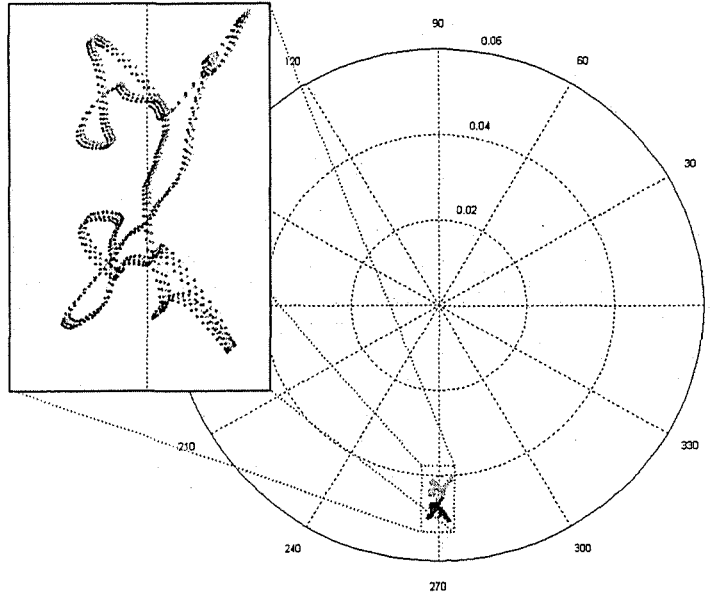


**Figure 16: Quasi-Frozen Orbit Condition**

## CONCLUSIONS

In its  $\Delta V$  budget, LRO has 150 m/s allocated to stationkeeping for a one year nominal mission duration. As demonstrated through analysis, this allocation is sufficient to meet the five mission constraints for stationkeeping maneuvers. The stationkeeping algorithm uses the natural dynamics of the non-spherical gravity of the moon to bound the altitude variation and minimized the stationkeeping  $\Delta V$ . In order to maintain the low lunar polar orbit with a mean altitude of 50 km, LRO will perform a pair of stationkeeping maneuvers every sidereal period, rotating the line-of-apsides and resetting the  $e$  vs.  $\omega$  pattern each period. These maneuvers are optimized by using the high orbit transfer at a LLAN of 270 deg.

## ACKNOWLEDGEMENTS

The authors would like to thank Farheen Rizvi, NASA Academy, for her help in performing analysis and generating many of the plots shown in this paper.

## REFERENCES

1. D. Folta, et. al., "Lunar Prospector Mission: Results of Trajectory Design, Quasi-Frozen Orbits, Extended Mission Targeting, and Luna Topography and Potential Models", AAS-99-397, Astrodynamics Specialist Conference, Girdwood, AK.1999.
2. A. Konopliv, et. al., "Recent Gravity Models as a Result of the Lunar Prospector Mission", Icarus vol. 150 no. 1 pp. 1-18, Pasadena, CA. 2001.
3. M. Beckman & D. Folta, "Mission Design of the First Robotic Lunar Exploration Program Mission: The Lunar Reconnaissance Orbiter", AAS-05-300, AAS/AIAA Astrodynamics Specialists Conference, Lake Tahoe, CA. 2005
4. D. Folta & D. Quinn, "Lunar Frozen Orbits", AAS/AIAA Astrodynamics Specialist Conference, Keystone, CO. 2006.